# Changing topographic *Hox* expression in blood vessels results in regionally distinct vessel wall remodeling

Nathanael D. Pruett[1], Zoltan Hajdu[2], Jing Zhang[2], Richard P. Visconti[2], Michael J. Kern[2], Deneen M. Wellik[3], Mark W. Majesky[4] and Alexander Awgulewitsch[1,*]

[1]Department of Medicine and [2]Department of Regenerative Medicine and Cell Biology, Medical University of South Carolina, Charleston, SC 29425, USA
[3]Division of Molecular Medicine and Genetics, Department of Internal Medicine, University of Michigan, Ann Arbor, MI 48109, USA
[4]Seattle Children's Research Institute, Departments of Pediatrics and Pathology, University of Washington, Seattle, WA 98101, USA
*Author for correspondence (awgulewa@musc.edu)

## Summary

The distinct topographic *Hox* expression patterns observed in vascular smooth muscle cells (VSMCs) of the adult cardiovascular system suggest that these transcriptional regulators are critical for maintaining region-specific physiological properties of blood vessels. To test this proposition, we expanded the vascular *Hoxc11* expression domain normally restricted to the lower limbs by utilizing an innovative integrated tetracycline regulatory system and *Transgelin* promoter elements to induce *Hoxc11* expression universally in VSMCs of transgenic mice. Ectopic *Hoxc11* expression in carotid arteries, aortic arch and descending aorta resulted in drastic vessel wall remodeling involving elastic laminae fragmentation, medial smooth muscle cell loss, and intimal lesion formation. None of these alterations were observed upon induction of *Hoxc11* transgene expression in the femoral artery, i.e. the natural *Hoxc11* activity domain, although this vessel was greatly enlarged, comparable to the topographically restricted vascular changes seen in *Hoxc11*$^{-/-}$ mice. To begin defining *Hoxc11*-controlled pathways of vascular remodeling, we performed immunolabeling studies in conjunction with co-transfection and chromatin immunoprecipitation (ChIP) assays using mouse vascular smooth muscle (MOVAS) cells. The results suggest direct transcriptional control of two members of the *matrix metalloproteinase (Mmp)* family, including *Mmp2* and *Mmp9* that are known as key players in the inception and progression of vascular remodeling events. In summary, the severe vascular abnormalities resulting from the induced dysregulated expression of a *Hox* gene with regional vascular patterning functions suggest that proper *Hox* function and regulation is critical for maintaining vascular functional integrity.

Key words: *Hox*, Smooth muscle cells, Vascular, Positional identity, Vascular remodeling, Topographic gene expression

## Introduction

A VSMC fate map of the aorta and its main branches revealed that VSMCs originating from different sources (neural crest, secondary heart field, somites, mesangioblasts, proepicardium, splanchnic mesoderm, mesothelium) reside in distinct segments (Majesky, 2007). This inherent regional diversity may be viewed as superimposed on VSMC heterogeneity based on differentiation status during normal development, as well as phenotype modulation during vascular injury and disease (Gittenberger-de Groot et al., 1999; Owens et al., 2004; Rensen et al., 2007; Yoshida and Owens, 2005). Members of the conserved *Hox* family of transcriptional regulators known to specify positional identities during embryonic patterning through a *Hox* code (Kessel and Gruss, 1991; McGinnis and Krumlauf, 1992) qualify as prime candidates for determining and maintaining positional identities in the vascular system. This idea is supported by recent data demonstrating topographic *Hox* expression patterns with distinct boundaries in VSMCs and endothelial cells of adult blood vessels (Pruett et al., 2008); the spatial coordinates of these vascular *Hox* domains roughly correspond to the respective *Hox* domains during embryonic development (Pruett et al., 2008). These results are consistent with data obtained by gene expression profiling of cultured human fibroblasts derived from various anatomic sites indicating that topographic *Hox* expression signatures are retained to some degree in certain adult tissues (Chang et al., 2002; Rinn et al., 2006). *Hox* genes may thus be critical for regulating site-specific differentiation processes in adult tissues, including the vasculature.

As an initial step towards testing the functional significance of topographic *Hox* patterns in the cardiovascular system, we designed a new transgenic mouse model by using an innovative integrated Tet-regulatory system for inducing changes in vascular *Hox* expression. Our data show that universal induction of *Hoxc11* expression in VSMCs results in region-specific vascular remodeling responses involving distinct histological and

molecular changes. These results suggest that properly regulated *Hox* activity patterns are critical for maintaining vessel wall homeostasis in a region-specific manner. This has important implications for the development of vascular diseases that exhibit topographic patterns.

## Results and Discussion

To induce changes to the distinct vascular *Hoxc11* expression pattern normally restricted to the lower hindlimb vessels (Pruett et al., 2008) we used an integrated tetracycline (Tet)-regulatory system (Bäckman et al., 2004) and *Transgelin (Tagln)* promoter elements that drive expression preferentially in VSMCs (Li et al., 1996). Profound morphological changes in the vasculature of male doxycycline (dox) –treated TetOn*(Tagln-Hoxc11)* mice (n=3) (Fig. 1F–I) compared to controls (Fig. 1B–E) were found by histopathological analysis of anatomically distinct vessel segments (external carotid artery, aortic arch, thoracic aorta, and femoral artery). Vessel wall remodeling in dox-induced mice was indicated by fragmentation of the elastic lamellae in the tunica media layer of anterior vessels including carotid artery, aortic arch, and thoracic aorta (Fig. 1F–H). In addition, intimal lesions were observed in carotid artery segments (asterisk, Fig. 1F) while medial lesions at the adventitial interface were observed in the aortic arch and thoracic aorta (black arrows, Fig. 1G,H). In contrast, the femoral artery of dox-induced mice exhibited no overt remodeling events in the vessel wall (Fig. 1I). Morphometric analysis of these vessels revealed significant
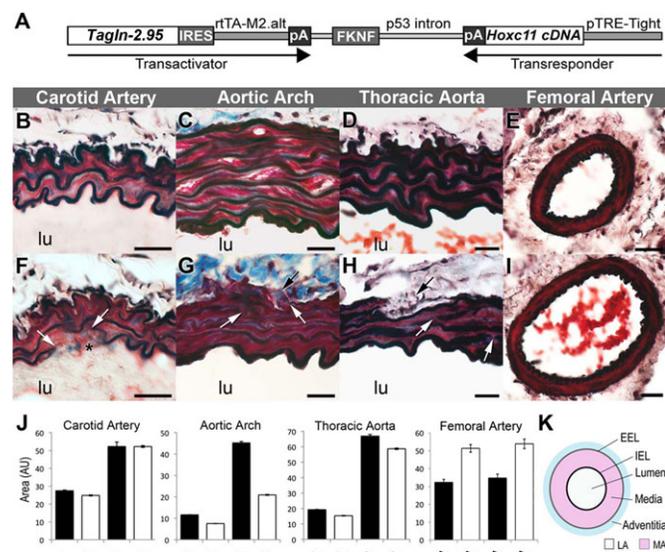
differences in medial area (MA) and luminal area (LA) between the two groups with the exception of the carotid artery (Fig. 1J,K). Mean area values of dox-induced aortic arch MA and LA were lower by 35.1% and 53.7%, respectively (ANOVA, $F_{(2,35)}=2358$, $P<0.0001$), and dox-induced thoracic aorta MA and LA were lower by 20.3% and 12.3%, respectively (ANOVA, $F_{(2,35)}=2030$, $P<0.0001$); the reduction of the medial areas of these two large arteries suggests a loss of vascular smooth muscle cells (VSMCs). In contrast, the femoral artery of dox-induced mice exhibited increases in both MA and LA mean values as compared to controls of 59.0% and 55.2%, respectively, (Fig. 1J,K) [ANOVA, $F_{(2,35)}=25.3$, $P<0.0001$].

Potential co-expression of molecular markers for vascular remodeling including MMP2, MMP9 (Raffetto and Khalil, 2008) and CASP3 (Ono et al., 2005) with HOXC11 upon TetOn*(Tagln-Hoxc11)* induction in the thoracic aorta and in femoral artery was examined by immunolabeling. The results indicate co-localization of HOXC11 with MMP2 and MMP9 in VSMCs (white arrows) and endothelial cells (grey arrows, Fig. 2B–D and Fig. 2J–L, respectively) of the thoracic aorta following one week of dox treatment, whereas in control sections HOXC11 expression was not detected (Fig. 2G,O). Faint signal for MMP2 was detectable in control sections where it localized to the periphery of elastic lamellae (green arrow, Fig. 2H) while signal for MMP9 was absent in the controls (Fig. 2P). Following a short three-day dox treatment, CASP3 was detectable in VSMCs adjacent to the intimal and adventitial interfaces and endothelial cells (large and small black arrows, respectively, Fig. 2Q) that was not detected in the controls (Fig. 2R); analysis of CASP3 expression was done after a three-day dox treatment as this is an early event in vascular remodeling (Spiguel et al., 2010).
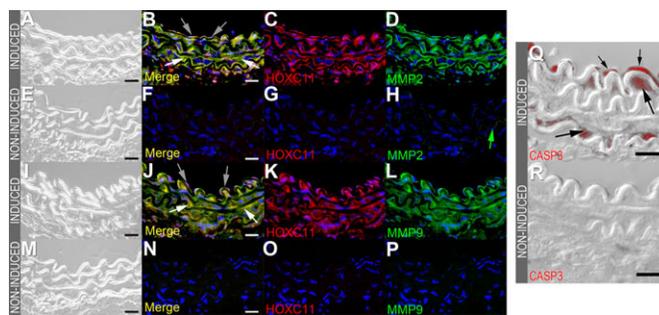


**Fig. 1. HOXC11-induced vessel wall restructuring.** (**A**) Schematic of the integrated dox-regulated transgene construct TetOn(*Tagln-Hoxc11*). (**B–E**) Cross-sections of arteries from four different anatomical locations: carotid artery, aortic arch, thoracic aorta and femoral artery (as indicated at the top of the panels) of TetOn(*Tagln-Hoxc11*) transgenic mice without dox treatment (controls). (**F–I**) Sections of arteries from dox-treated transgenic mice that match those shown in panels B-E; white arrows in (F,G,H) indicate fragmented elastic lamellae; asterisk (F) indicates intimal lesion; black arrows (G,H) identify medial lesions; lu, lumen; scale bars: 20 µm. (**J,K**) Morphometric analysis of medial area (MA) and luminal area (LA) of un-induced (UI) versus induced (IN) vessel segments (carotid artery, aortic arch, thoracic aorta, femoral artery) as schematically depicted in the cartoon (panel K) and explained in the text; values are expressed as mean ±SEM, n=9; $P<0.001$ in all cases.



**Fig. 2. MMP2/MMP9 and CASP3 expression in thoracic aorta upon TetOn(*Tagln-Hoxc11*) induction.** (**A–D**) Thoracic aorta cross section from dox-induced (1 week) TetOn(*Tagln-Hoxc11*) transgenic mouse imaged with differential interference contrast (DIC; panel A) showing co-expression (merge; yellow signal in panel B) of individual immunofluorescent signals for HOXC11 and MMP2 (C and D, respectively). (**E–H**) In cross-section of un-induced counterpart HOXC11 expression was not detected (G) and MMP2 signal was barely detectable (green arrow; panel H). (**I–L**) Thoracic aorta cross section from an induced transgenic mouse imaged with DIC (panel I) showing co-expression (yellow signal; panel J) of individual immunofluorescent signals for HOXC11 and MMP9 (K and L, respectively). (**M–P**) Thoracic aorta cross-section of un-induced counterpart indicated lack of HOXC11 and MMP9 expression. (**Q,R**) Immunofluorescent signals for CASP3 (red) were superimposed on DIC images of induced (Q) and un-induced thoracic aorta (R) indicating increased apoptosis in dox-induced (3 days) mouse vessel. All vessel segments were harvested and processed in parallel. Imaging was performed on an upright brightfield/fluorescence microscope (Leica DMR) equipped a SPOT RT3 camera and SPOT v4.6.1.40 imaging software. Scale bars: 20 µm.
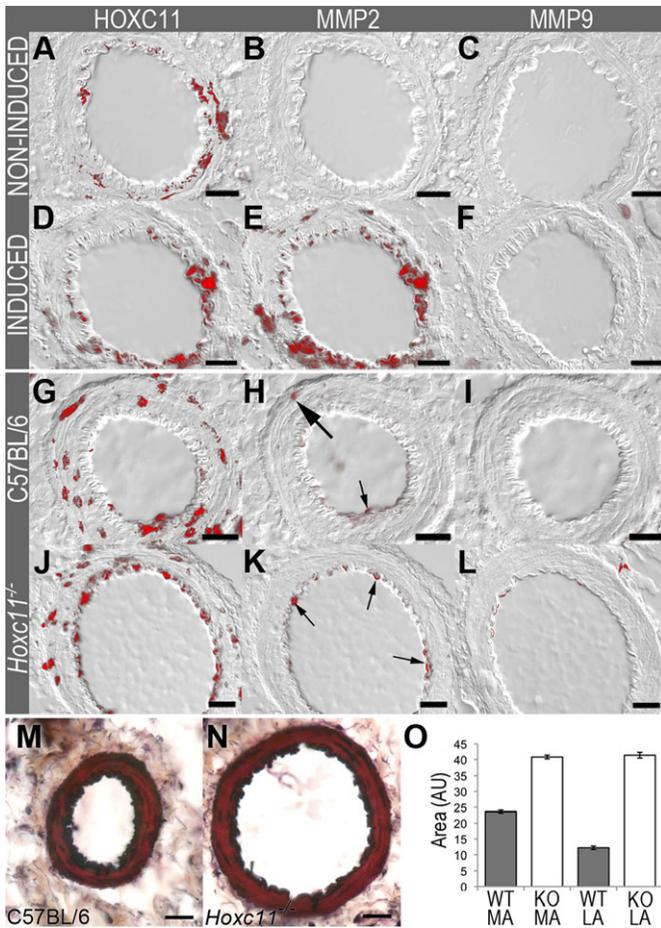
**Fig. 3. Changes in femoral artery of dox-induced TetOn(*Tagln-Hoxc11*) transgenic and *Hoxc11⁻/⁻* knockout mice. (A–C)** Femoral artery sections (FAS) of a non-induced transgenic mouse immunolabeled with HOXC11, MMP2 and MMP9 antibodies as indicated at the top reveal HOXC11 expression (red signal; panel A); FAS of dox-induced (3 days) transgenic mouse (**D–F**) show in addition to HOXC11 expression (D) induced expression of MMP2 (E) in a largely similar pattern. (**G–I**) In a separate experiment, FAS of wild type C57BL/6 mouse immunolabeled with HOXC11, MMP2 and MMP9 antibodies show HOXC11 expression (G) and faint MMP2 expression signals (arrows in H); (**J–L**) FAS of *Hoxc11⁻/⁻* mouse show expression of truncated HOXC11 (J) and faint MMP2 expression (arrows in I). (**M,N**) Movat's pentachrome-stained FAS from wild type (WT) (M) and *Hoxc11⁻/⁻* mice (N). (**O**) Morphometric analysis of medial area (MA) and luminal area (LA) of wild-type (WT) versus *Hoxc11⁻/⁻* FAS; values and comparisons (explained in text) are expressed as mean ±SEM, n=9; *P*<0.001. Scale bars: 20 μm.

Expectedly, HOXC11 was detected in distal femoral arteries of both induced and non-induced mice (red signal, Fig. 3A,D), respectively, with a concomitant induction of MMP2 in induced animals (red signal, Fig. 3E) that was absent in the controls (Fig. 3B). Since we cannot discriminate between endogenous and transgene-induced HOXC11, we conclude that the MMP2 induction in dox-treated mice resulted from increased levels of HOXC11 expression (supplementary material Fig. S1). No signal for MMP9 expression was detected in either group (induced or non-induced) (Fig. 3C,F) respectively.

To determine potential changes in the femoral artery of *Hoxc11⁻/⁻* mice that might reveal a role for *Hoxc11* in vascular patterning during development, we performed a limited histopathological analysis of these mice. Morphometric measurements of medial and luminal femoral artery areas (MA and LA, respectively) from *Hoxc11⁻/⁻* mice and wild-type littermates (n=3) at 6 weeks of age showed remarkable increases of 72.6% in MA and 239% in LA for *Hoxc11⁻/⁻* compared to control mice (Fig. 3M–O) [ANOVA, $F_{(3,39)}$=476.3, *P*<0.0001]. Interestingly, this vessel enlargement is accompanied by transformations of sacral (S) and caudal (C) vertebrae from posterior towards anterior identities, including S3 to S2 and C1 to S4 transformations (supplementary material Fig. S2) that may be considered classic homeotic transformations as expected from the inactivation of *AbdB*-type ("posterior") *Hox* genes (Gehring, 1987; Lewis, 1978; Mallo et al., 2010; Wellik, 2007). This raises an intriguing question, i.e. whether the femoral artery enlargement in *Hoxc11⁻/⁻* mice might conceptually also be viewed as a homeotic transformation, in this case from distal vessel of smaller size towards a larger more proximal vessel; addressing this will be the focus of future studies. Although this vessel enlargement superficially resembled the enlargement observed in dox-treated TetOn(*Tagln-Hoxc11*) transgenic mice, where this was accompanied by the induction of robust MMP2 expression (Fig. 3E), the comparatively weak MMP2 expression detected in femoral artery VSMCs and endothelial cells of *Hoxc11⁻/⁻* mice (Fig. 3K) was essentially indistinguishable from wild type (Fig. 3H), and MMP9 expression was undetectable in both (Fig. 3F,L). Interestingly, the mosaic expression pattern of truncated and native HOXC11 in the femoral artery of *Hoxc11⁻/⁻* and wild type mice, respectively, was essentially the same (Fig. 3G,J); the epitope recognized by the anti-HOXC11 antibodies is exon 1-specific, while the targeted alteration of HOXC11 disrupts exon 2 (Wellik et al., 2002) thus allowing for detection of the truncated protein.

The presence of multiple copies of the TTTA(T/C) HOXC11 consensus binding sequence (Sur and Toftgård, 2000) within the *Mmp2* and *Mmp9* promoter regions (Fig. 4A) suggests potential direct regulatory interactions with HOXC11. To test this, we performed chromatin immunoprecipitation (ChIP) assays with MOVAS cells transiently transfected with a plasmid encoding a FLAG-tagged (N-terminal) version of HOXC11 (F-HOXC11); endogenous *Hoxc11* expression was not detected in MOVAS cells by semi-quantitative PCR (supplementary material Fig. S3). Immunoprecipitated chromatin fragments (anti-FLAG) yielded *Mmp2* and *Mmp9*-specific amplicons of expected sizes upon PCR amplification not observed with the control reactions (Fig. 4B). To further validate HOXC11 interaction with *Mmp2* and *Mmp9* promoters, we performed co-transfection assays with MOVAS cells utilizing HOXC11 expression plasmids encoding either full-length HOXC11 or a homeodomain-deleted version of HOXC11 (HOXC11Δhd) and FLAG-tagged versions of both (F-HOXC11 and F-HOXC11Δhd) along with *Mmp2*- and *Mmp9*-luciferase (*Mmp2*- and *Mmp9*-luc) reporter plasmids containing 2.7 and 1.9 kb of respective proximal promoter sequences (Fig. 4A). Cells co-transfected with vehicle plus *Mmp2*-luc or *Mmp9*-luc (controls) showed considerable basal levels of luciferase activity (Fig. 4C,D) consistent with recent reports showing MMP2 and MMP9 to be expressed in aortic ring VSMC primary cultures (Dwivedi et al., 2009; Risinger et al., 2010); in addition, *Mmp9* is specifically expressed in MOVAS cells (Lau et al., 2009). Co-transfection of *Mmp2*-luc with HOXC11 or F-HOXC11 resulted in significant inhibition of luciferase activity, 3.80-fold and 4.66-fold, respectively (Fig. 4C) [ANOVA, $F_{(4,29)}$=280.9, *P*<0.0001]. Significantly reduced inhibition was found upon

co-transfection with HOXC11Δhd and F-HOXC11Δhd, 2.24-fold and 1.83-fold, respectively. An analogous set of co-transfection assays with *Mmp9*-luciferase yielded overall very similar results although with an even greater degree of inhibition associated with co-expression with HOXC11 and F-HOXC11, 7.88-fold and 12.89-fold respectively (Fig. 4D) [ANOVA, $F_{(4,44)}=125.5$, $P<0.0001$]. An even greater release of inhibition was observed upon co-transfection with HOXC11Δhd and F-HOXC11Δhd,
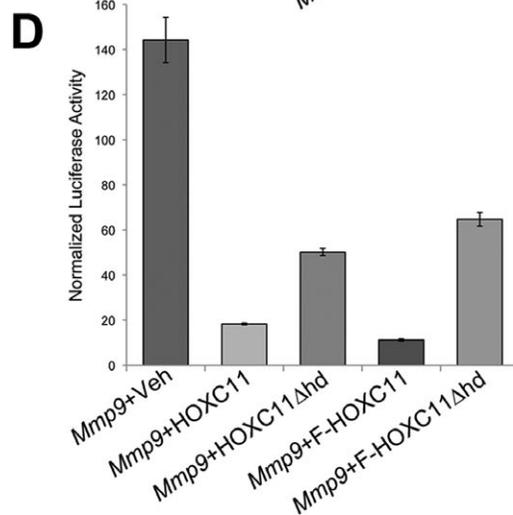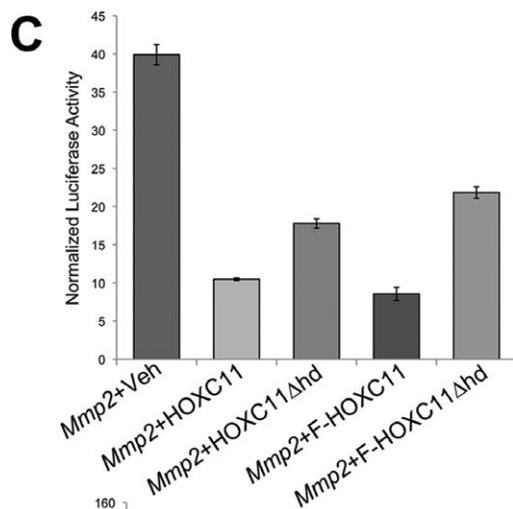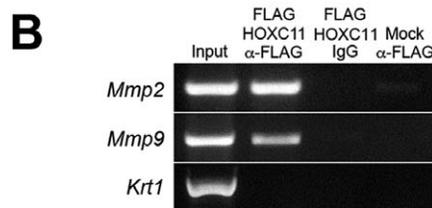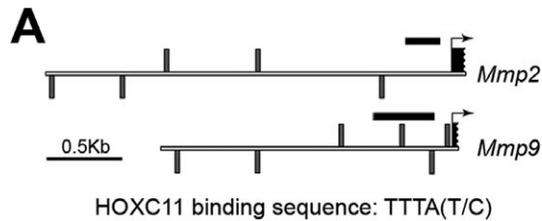


2.87-fold and 2.23-fold, respectively (Fig. 4D), $P<0.0001$. These results are consistent with the non-normalized set of data for these same experiments as both show the same trends in luciferase activities (compare Fig. 4 to supplementary material Fig. S4); this is an important observation as interference with the expression of the control reporter plasmid can result in biased interpretation of the normalized data (Vesuna et al., 2005). A possible explanation for the opposing effects of HOXC11 expression on *Mmp2* and *Mmp9* reporter gene activity in MOVAS cells and the apparent induction of MMP2 and MMP9 expression upon HOXC11 activity *in vivo* is that plasmid-based reporter gene expression in cultured cells is unlikely to reflect authentic responses of the corresponding genes in their native cellular and nuclear environment.

While induction of TetOn(*Tagln-Hoxc11*) activity outside the normal *Hoxc11* expression domain (Pruett et al., 2008) resulted in rather uniform HOXC11 expression in the vessel walls as judged by immunolabeling (Fig. 2), this was not the case in the femoral artery, where HOXC11 expression appeared in a mosaic pattern (Fig. 3) that resembled the endogenous pattern (Fig. 3) (Pruett et al., 2008). This is likely to reflect phenotypic heterogeneity among VSMCs and suggests regulatory mechanisms selectively suppressing TetOn(*Tagln-Hoxc11*) activity in certain cells. A possible explanation includes the involvement of other topographically expressed transcription factors (e.g. the *AbdB*-type *Hoxc9, Hoxc10, Hoxd10,* and *Hoxa11*) that are expressed in the same vessel segment as *Hoxc11* (Pruett et al., 2008) but not necessarily in the same cells. In support of this idea, *in silico* analysis of the *Tagln* promoter sequences present in TetOn(*Tagln-Hoxc11*) revealed the presence of 13 *bona fide* AbdB-type HOX binding sequences (Benson et al., 1995) that could mediate this selective transgene repression.

We demonstrate that dysregulated expression of *Hoxc11* in adult arteries resulted in profound vascular remodeling with distinct regionally restricted morphological and molecular changes. Ectopic expression in the large arteries (external carotids, aortic arch and thoracic aorta) was marked by fragmentation of elastic laminae, loss of VSMCs and formation of intimal lesions as reflected by the induction of MMP2, MMP9, and CASP3 activity. In contrast, induction of TetOn(*Tagln-Hoxc11*) activity within the endogenous vascular *Hoxc11* domain, as illustrated by the analysis of the femoral artery, resulted in approximately 2-fold enlargement of this vessel but without overtly recognizable changes in vessel wall structure, and without MMP9 and CASP3 induction. This differential response

**Fig. 4. HOXC11 interaction with *Mmp2* and *Mmp9* promoters.**
(**A**) Schematic of *Mmp2* and *Mmp9* proximal promoter regions with the positions of HOXC11 consensus binding sequences [TTTA(T/C)] indicated by vertical bars. Location of PCR amplicons used for detecting immunoprecipitated chromatin are shown by horizontal black bars. (**B**) ChIP assays using MOVAS cells transfected with FLAG-tagged HOXC11 (F-HOXC11); PCR amplification of chromatin fragments precipitated with anti-FLAG antibodies (a-FLAG) yielded gene-specific amplicons for both *Mmp2* and *Mmp9* but not for *Krt1* used as negative control; PCR reactions using chromatin precipitated with pre-immune rabbit IgG and with a-FLAG/ Mock (vehicle-only) failed to produce promoter-specific amplicons in all cases. (**C,D**) HOXC11 inhibits the luciferase activity of reporter vectors carrying the *Mmp2* and *Mmp9* promoter sequences as depicted above (A); histograms of normalized luciferase activity of MOVAS cells co-transfected with *Mmp2-* (C) and *Mmp9*-luciferase (D) vectors and vectors encoding either HOXC11, HOXC11 minus the homeodomain (HOXC11ΔHD), FLAG-tagged HOXC11 (F-HOXC11) or FLAG-tagged HOXC11 minus the homeodomain (F-HOXC11ΔHD) 48 hours prior to measuring luciferase activity.

to TetOn(*Tagln-Hoxc11*) activation supports our idea that *Hox*-specified positional identity is both retained and functional in the adult arterial system. Conceptually, this may be viewed as a vascular *Hox* code that provides the genetic basis for maintaining vessel wall homeostasis and functional diversity.

This new concept has potential clinical relevance as illustrated by data that indicate topographic patterns in the development of various vascular diseases. A good example is the localized formation of abdominal aortic aneurysms (AAA) whose formation involve genetic mechanisms that are distinct from those that underlie thoracic aortic aneurysms (Lindsay and Dietz, 2011); within this context it is of interest that AAA is associated with loss of *HOXA4* expression (Lillvis et al., 2011). Furthermore, the finding of distinct topographic variations in the development of arterial occlusive disease in spite of uniform systemic risk factors (sex, cholesterol, triglyceride levels, smoking, hypertension) was thought to indicate genetic differences in the arterial bed (DeBakey and Glaeser, 2000). This idea is consistent with data that showed a clear propensity for atherosclerotic lesion progression at the left anterior descending coronary artery compared to the thoracic and abdominal aorta (Homma et al., 2008). Finally, CpG islands associated with *HOXC11* were found to be hypomethylated in human atherosclerotic coronary arteries suggesting ectopic activation of this gene during atherosclerotic lesion formation (Castillo-Díaz et al., 2010); this finding is consistent with the vessel wall restructuring induced by ectopic *Hoxc11* expression in mice presented here.

## Materials and Methods

### HOXC11 expression vectors and luciferase reporter constructs
*Hoxc11* coding sequence (cds) was isolated by PCR from an E16 mouse embryo (FVB/N) cDNA library generated with SuperScript® III (Invitrogen, Carlsbad, CA); primer pair: 5′-CCGGAGGAGGCAGGAGAAGA and 5′-TCTTTCCCTCCCTCCCACCCCAAA; the subcloned cds (TOPO TA Kit, Invitrogen) was excised (*EcoRI*) and cloned into pCDNA3.1+ (Invitrogen) to generate pHOXC11; alternatively, blunt-ended cds was cloned into the end-filled *BamHI* site of a FLAG-tagged version of pCDNA3.1+ (Potter et al., 2006) to generate pF-HOXC11. Homeodomain (hd) -deleted versions of these vectors (pHOXC11Δhd and pF-HOXC11Δhd) were generated by removal of an *Eco47III-XhoI* fragment encoding hd residues 4–60. *Mmp2* and *Mmp9* promoter regions were isolated by PCR from BAC clones RP24-138B4 and RP24-320F19 (CHORI, Oakland CA), respectively, using Expand High Fidelity^PLUS System (Roche, Indianapolis, IN) with specific primer pairs as listed in supplementary material Table S1; forward and reverse primers included an Mlu1 and Xho site, respectively, thus facilitating cloning into pGL2-Basic containing *Photinus pyralis* luciferase sequences (Promega, Madison, WI) to generate p*Mmp2-luc* and p*Mmp9-luc*.

### Transgenic and knockout mice
The *Tagln* promoter harbored in pSM22#43 vector (Li et al., 1996) was inserted into the end-filled *XhoI* site of pe2TetOnFKNF(PacI) (Bäckman et al., 2004) to generate pe2TetOn(*Tagln*2.7); the *Hoxc11* coding sequence (cds) excised from pHOXC11 was inserted into the *PacI* site of pe2TetOn(*Tagln*2.7) to generate pTetOn(*Tagln-Hoxc11*). TetOn(*Tagln-Hoxc11*) transgenic mice were created on an inbred FVB/N strain background as described (Gordon and Ruddle, 1983). Transgene activity was induced at 6–8 weeks of age by supplementing the drinking water with 3% sucrose and 500 μg/ml of doxycycline exchanged every third day. *Hoxc11*^−/− mice were described previously (Wellik et al., 2002).

### Blood vessel dissection and histological analysis
Defined blood vessel segments of dox-treated (2 weeks) and non-treated TetOn(*Tagln-Hoxc11*) mice (n=3) were dissected (carotid artery: within 1 mm anterior of the internal/external carotid branch point; aortic arch: transverse-midpoint between left carotid and innominate arterial branches; thoracic aorta: between 7th and 8th intercostal arterial branch points; femoral artery: within 1 mm anterior of the tibial artery branch point). Morphometric measurements of three randomly selected, histologically stained (Movat's pentachrome staining kit; Electron Microscopy Services, Hatfield, PA) and digitally imaged sections were

performed by using ImageJ software v1.4 (http://rsb.info.nih.gov/ij/) as described (Moore and Hui, 2005).

### Immunolabeling
Immunolabeling was performed as described (Pruett et al., 2008) by using chicken-anti-mouse HOXC11(Pruett et al., 2008); rabbit-anti-human/mouse MMP2 (AB19167; Millipore, Temecula, CA), rabbit-anti-rat/mouse MMP9 (AB19016; Millipore, Temecula, CA), and rabbit-anti-human/mouse CASP3 (ab13847; Abcam, Cambridge, MA) antibodies.

### ChIP and co-transfection assays
Assays were performed with MOVAS cells (ATCC, Rockville, MD) by using the ChIP-IT Express Enzymatic kit (Active Motif, Carlsbad, CA) and Luciferase Assay System (Promega, Madison WI) according to manufacturer's instructions and as previously reported (Potter et al., 2006). For ChIP, anti-FLAG antibodies (Sigma, St. Louis, MO) were used and precipitated chromatin samples were amplified by PCR (35 cycles) using primer pairs specific for *Mmp2, Mmp9,* and *Krt1* promoter regions as listed in supplementary material Table S1.

### Statistical analysis
In all cases ANOVA analysis (one-way) with subsequent Student-Newman-Keul's Test *post hoc* analysis was used for comparisons of means between groups with statistical significance set at the $P<0.05$ level.

### Methods used for supplementary material Fig. S1
Total RNA of mouse femoral artery and carotid artery was isolated using the RNeasy Mini Kit (Qiagen, Valencia, CA), and cDNA was generated from 200 ng of total RNA using SuperScript III RNase H reverse transcriptase with random primers (Invitrogen, Carlsbad, CA). Q-PCR reactions were performed by using RT″ PCR SYBR® Green Mastermix (Qiagen) and *Hoxc11* forward and reverse primers 5′-AGGCTCCCTCTCGTCAGATTT and 5′-CTCCCGGTGCATAAG-CTCG, respectively, on a BIO-RAD (Hercules, CA) MyiQ thermocycler. Mouse *Gapdh* forward and reverse primers: 5′-TGTTCCTACCCCCAATGTGT, and 5′-GGTCCTCAGTGTAGCCCAAG.

## Competing Interests
The authors declare that there are no competing interests.

## References
**Bäckman, C. M., Zhang, Y., Hoffer, B. J. and Tomac, A. C.** (2004). Tetracycline-inducible expression systems for the generation of transgenic animals: a comparison of various inducible systems carried in a single vector. *J. Neurosci. Methods* **139**, 257-262.

**Benson, G. V., Nguyen, T. H. and Maas, R. L.** (1995). The expression pattern of the murine Hoxa-10 gene and the sequence recognition of its homeodomain reveal specific properties of Abdominal B-like genes. *Mol. Cell. Biol.* **15**, 1591-1601.

**Castillo-Díaz, S. A., Garay-Sevilla, M. E., Hernández-González, M. A., Solís-Martínez, M. O. and Zaina, S.** (2010). Extensive demethylation of normally hypermethylated CpG islands occurs in human atherosclerotic arteries. *Int. J. Mol. Med.* **26**, 691-700.

**Chang, H. Y., Chi, J. T., Dudoit, S., Bondre, C., van de Rijn, M., Botstein, D. and Brown, P. O.** (2002). Diversity, topographic differentiation, and positional memory in human fibroblasts. *Proc. Natl. Acad. Sci. USA* **99**, 12877-12882.

**DeBakey, M. E. and Glaeser, D. H.** (2000). Patterns of atherosclerosis: effect of risk factors on recurrence and survival-analysis of 11,890 cases with more than 25-year follow-up. *Am. J. Cardiol.* **85**, 1045-1053.

**Dwivedi, A., Slater, S. C. and George, S. J.** (2009). MMP-9 and -12 cause N-cadherin shedding and thereby beta-catenin signalling and vascular smooth muscle cell proliferation. *Cardiovasc. Res.* **81**, 178-186.

**Gehring, W. J.** (1987). Homeo boxes in the study of development. *Science* **236**, 1245-1252.

**Gittenberger-de Groot, A. C., DeRuiter, M. C., Bergwerff, M. and Poelmann, R. E.** (1999). Smooth muscle cell origin and its relation to heterogeneity in development and disease. *Arterioscler. Thromb. Vasc. Biol.* **19**, 1589-1594.

**Gordon, J. W. and Ruddle, F. H.** (1983). Gene transfer into mouse embryos: production of transgenic mice by pronuclear injection. *Methods Enzymol.* **101**, 411-433.

**Homma, S., Troxclair, D. A., Zieske, A. W., Malcom, G. T. and Strong, J. P.**; Pathobiological Determinants of Atherosclerosis in Youth (PDAY) Research Group. (2008). Histological topographical comparisons of atherosclerosis progression in juveniles and young adults. *Atherosclerosis* **197**, 791-798.

**Hostikka, S. L., Gong, J. and Carpenter, E. M.** (2009). Axial and appendicular skeletal transformations, ligament alterations, and motor neuron loss in Hoxc10 mutants. *Int. J. Biol. Sci.* **5**, 397-410.

**Kessel, M. and Gruss, P.** (1991). Homeotic transformations of murine vertebrae and concomitant alteration of Hox codes induced by retinoic acid. *Cell* **67**, 89-104.

**Lau, A. C., Duong, T. T., Ito, S., Wilson, G. J. and Yeung, R. S.** (2009). Inhibition of matrix metalloproteinase-9 activity improves coronary outcome in an animal model of Kawasaki disease. *Clin. Exp. Immunol.* **157**, 300-309.

**Lewis, E. B.** (1978). A gene complex controlling segmentation in Drosophila. *Nature* **276**, 565-570.

**Li, L., Miano, J. M., Mercer, B. and Olson, E. N.** (1996). Expression of the SM22alpha promoter in transgenic mice provides evidence for distinct transcriptional regulatory programs in vascular and visceral smooth muscle cells. *J. Cell Biol.* **132**, 849-859.

**Lillvis, J. H., Erdman, R., Schworer, C. M., Golden, A., Derr, K., Gatalica, Z., Cox, L. A., Shen, J., Vander Heide, R. S., Lenk, G. M. et al.** (2011). Regional expression of HOXA4 along the aorta and its potential role in human abdominal aortic aneurysms. *BMC Physiol.* **11**, 9.

**Lindsay, M. E. and Dietz, H. C.** (2011). Lessons on the pathogenesis of aneurysm from heritable conditions. *Nature* **473**, 308-316.

**Majesky, M. W.** (2007). Developmental basis of vascular smooth muscle diversity. *Arterioscler. Thromb. Vasc. Biol.* **27**, 1248-1258.

**Mallo, M., Wellik, D. M. and Deschamps, J.** (2010). Hox genes and regional patterning of the vertebrate body plan. *Dev. Biol.* **344**, 7-15.

**McGinnis, W. and Krumlauf, R.** (1992). Homeobox genes and axial patterning. *Cell* **68**, 283-302.

**Moore, Z. W. and Hui, D. Y.** (2005). Apolipoprotein E inhibition of vascular hyperplasia and neointima formation requires inducible nitric oxide synthase. *J. Lipid Res.* **46**, 2083-2090.

**Ono, H., Ichiki, T., Ohtsubo, H., Fukuyama, K., Imayama, I., Hashiguchi, Y., Sadoshima, J. and Sunagawa, K.** (2005). Critical role of Mst1 in vascular remodeling after injury. *Arterioscler. Thromb. Vasc. Biol.* **25**, 1871-1876.

**Owens, G. K., Kumar, M. S. and Wamhoff, B. R.** (2004). Molecular regulation of vascular smooth muscle cell differentiation in development and disease. *Physiol. Rev.* **84**, 767-801.

**Potter, C. S., Peterson, R. L., Barth, J. L., Pruett, N. D., Jacobs, D. F., Kern, M. J., Argraves, W. S., Sundberg, J. P. and Awgulewitsch, A.** (2006). Evidence that the satin hair mutant gene Foxq1 is among multiple and functionally diverse regulatory targets for Hoxc13 during hair follicle differentiation. *J. Biol. Chem.* **281**, 29245-29255.

**Pruett, N. D., Visconti, R. P., Jacobs, D. F., Scholz, D., McQuinn, T., Sundberg, J. P. and Awgulewitsch, A.** (2008). Evidence for Hox-specified positional identities in adult vasculature. *BMC Dev. Biol.* **8**, 93.

**Raffetto, J. D. and Khalil, R. A.** (2008). Matrix metalloproteinases and their inhibitors in vascular remodeling and vascular disease. *Biochem. Pharmacol.* **75**, 346-359.

**Rensen, S. S. M., Doevendans, P. A. F. M. and van Eys, G. J. J. M.** (2007). Regulation and characteristics of vascular smooth muscle cell phenotypic diversity. *Neth. Heart J.* **15**, 100-108.

**Rinn, J. L., Bondre, C., Gladstone, H. B., Brown, P. O. and Chang, H. Y.** (2006). Anatomic demarcation by positional variation in fibroblast gene expression programs. *PLoS Genet.* **2**, e119.

**Risinger, G. M., Jr, Updike, D. L., Bullen, E. C., Tomasek, J. J. and Howard, E. W.** (2010). TGF-beta suppresses the upregulation of MMP-2 by vascular smooth muscle cells in response to PDGF-BB. *Am. J. Physiol. Cell Physiol.* **298**, C191-C201.

**Spiguel, L. R., Chandiwal, A., Vosicky, J. E., Weichselbaum, R. R. and Skelly, C. L.** (2010). Concomitant proliferation and caspase-3 mediated apoptosis in response to low shear stress and balloon injury. *J. Surg. Res.* **161**, 146-155.

**Sur, I. P. and Toftgård, R.** (2000). Repression of transcription by HoxC11 upon phorbol ester stimulation. *Mol. Cell Biol. Res. Commun.* **3**, 367-373.

**Vesuna, F., Winnard, P. and Jr and Raman, V.** (2005). Enhanced green fluorescent protein as an alternative control reporter to Renilla luciferase. *Anal. Biochem.* **342**, 345-347.

**Wellik, D. M.** (2007). Hox patterning of the vertebrate axial skeleton. *Dev. Dyn.* **236**, 2454-2463.

**Wellik, D. M., Hawkes, P. J. and Capecchi, M. R.** (2002). Hox11 paralogous genes are essential for metanephric kidney induction. *Genes Dev.* **16**, 1423-1432.

**Yoshida, T. and Owens, G. K.** (2005). Molecular determinants of vascular smooth muscle cell diversity. *Circ. Res.* **96**, 280-291.